International Journal of Heat and Mass Transfer 145 (2019) 118719

Contents lists available at ScienceDirect

International Journal of Heat and Mass Transfer

journal homepage: www.elsevier.com/locate/ijhmt

Thermal conductivity of molybdenum disulfide nanotube from molecular dynamics simulations

Han Meng [a], Dengke Ma [a,b], Xiaoxiang Yu [a], Lifa Zhang [b], Zhijia Sun [c], Nuo Yang [a,*]

[a] State Key Laboratory of Coal Combustion, School of Energy and Power Engineering, Huazhong University of Science and Technology, Wuhan 430074, China
[b] NNU-SULI Thermal Energy Research Center (NSTER) & Center for Quantum Transport and Thermal Energy Science (CQTES), School of Physics and Technology, Nanjing Normal University, Nanjing 210023, China
[c] Institute of High Energy Physics, Chinese Academy of Sciences, Beijing 100049, China

ARTICLE INFO

Article history:
Received 1 July 2019
Received in revised form 6 September 2019
Accepted 10 September 2019

Keywords:
Thermal conductivity
Molybdenum disulfide nanotube
Strain effect
Temperature dependence
Size effect
Molecular dynamics simulations

ABSTRACT

Single layer molybdenum disulfide ($SLMoS_2$), a semiconductor possesses intrinsic bandgap and high electron mobility, has attracted great attention due to its unique electronic, optical, mechanical and thermal properties. Although thermal conductivity of $SLMoS_2$ has been widely investigated recently, less studies focus on molybdenum disulfide nanotube (MoS_2NT). Here, the comprehensive temperature, size and strain effect on thermal conductivity of MoS_2NT are investigated. Thermal conductivity is obtained as 16 $Wm^{-1} K^{-1}$ at room temperature, and it has a $\sim T^{-1}$ dependence on temperature from 200 to 400 K and a $\sim L^{\beta}$ dependence on length from 10 to 320 nm. Interestingly, a chirality-dependent strain effect is identified in thermal conductivity of zigzag nanotube, in which the phonon group velocity can be significantly reduced by strain. This work not only provides feasible strategies to modulate the thermal conductivity of MoS_2NT, but also offers useful insights into the fundamental mechanisms that govern the thermal conductivity, which can be used for the thermal management of low dimensional materials in optical, electronic and thermoelectrical devices.

1. Introduction

In recent years, two-dimensional single layer molybdenum disulfide ($SLMoS_2$) with a tri-layer structure composed of one layer of Mo atoms sandwiched between two layers of S atoms, has attracted great attention due to its unique electronic [1], optical [2], and mechanical [3,4] properties. Different from the gapless conductor graphene, $SLMoS_2$ is a semiconductor with an intrinsic bandgap and high electron mobility [5], which makes it become a promising candidate for many electronic and optoelectronic applications [6–8]. However, thermal properties of low-dimensional systems are very important for the performance and reliability of devices. As a typical low-dimensional material, nanotubes have attracted increasing research interest due to their distinct thermal properties arising from the reduced dimensionality, increased quantum confinement, and surface phonon scatterings [9]. With the development of material science, quasi one-dimensional molybdenum disulfide nanotube (MoS_2NT) has been experimentally prepared [10,11].

During past years, thermal properties of $SLMoS_2$ have been widely studied recently [12–17]. Jin et al. calculated the thermal conductivity of $SLMoS_2$ using equilibrium molecular dynamics and reported a value of 116.8 $Wm^{-1} K^{-1}$ at room temperature [13]. Wu et al. studied the isotropic effect on the thermal conductivity of $SLMoS_2$ and found that Mo isotopes contribute more and can strongly scatter phonons with intermediate frequency for large size samples [14]. Ding et al. found that the thermal conductivity of $SLMoS_2$ can be effectively tuned by introducing even a small amount of lattice defects, and can be further tuned by mechanical strain [15]. In contrast, only a few researches focus on MoS_2NT. The mechanical behavior of MoS_2NT under compression, tension and torsion was studied [18]. Besides, the stability, thermal behavior and size dependence of thermal conductivity of MoS_2NT were investigated by molecular dynamics simulations [19]. However, the study on thermal conductivity of MoS_2NT is not enough, temperature, strain and chirality dependence of thermal conductivity are missing and the fundamental physical mechanism of thermal transport still remains to be revealed.

In this work, thermal conductivities of MoS_2NT is numerically investigated. Firstly, two different chiral MoS_2NTs with different sizes are constructed. Then, temperature, diameter and length dependence of thermal conductivity are studied for both two chiral

* Corresponding author.
E-mail address: nuo@hust.edu.cn (N. Yang).

https://doi.org/10.1016/j.ijheatmasstransfer.2019.118719
0017-9310/

MoS_2NT, as well as strain effect. Lastly, lattice dynamics analysis is carried out to explain the chirality-dependent strain effect on thermal conductivity by quantifying the phonon dispersion relations and group velocity.

2. Model and method

Different chiral MoS_2NT is constructed by rolling up $SLMoS_2$ based on specific lattice vector $\mathbf{r} = m\mathbf{a_1} + n\mathbf{a_2}$, where the lattice constants of the primitive cell are $a_1 = a_2 = 3.147$ Å (as shown in Fig. 1a). Since that armchair and zigzag are two most representative directions in two-dimensional material, armchair and zigzag nanotube have become the prevalent objects in the research on nanotube. Therefore, our study only focuses on armchair nanotube (ANT, m = n) and zigzag nanotube (ZNT, $m \neq 0$ and n = 0) without considering other chiral MoS_2NTs. For instance, Fig. 1b and c show the atomic structure of (8,8) ANT and the (14,0) ZNT respectively. To overcome the structural instability induced by small diameter, the (40, 40) ANT and (70, 0) ZNT are chosen as the smallest structure in the following calculation.

The classical non-equilibrium molecular dynamics (NEMD) method has been employed in the calculation of thermal properties [20–28]. The thermal conductivity is calculated based on the Fourier's law of heat conduction as

$$\kappa = -\frac{J}{A\nabla T}, \tag{1}$$

where A is the cross-sectional area, ∇T is the temperature gradient, J is the heat flux that recorded by the average of the input and output power of the two baths as

$$J = \frac{\Delta E_{in} + \Delta E_{out}}{2\Delta t}, \tag{2}$$

where ΔE is the energy added to or removed from each heat bath during each time step Δt.

All simulations are performed by the large-scale atomic/molecular massively parallel simulator (LAMMPS) package [29], which has been widely used to study thermal transport properties [30–34]. Stillinger-Weber potential includes both two-body and three-body terms and has been widely employed to calculate the thermal properties [35–39]. The interatomic interactions are described by the potential parameterized by Jiang, which has been successfully tested for thermal conductivity calculation of $SLMoS_2$ [40]. Time step is set as 0.5 fs, and the velocity Verlet algorithm is used to integrate the discrete differential equations of motion [41]. The fixed and periodic boundary conditions are applied in axial and other two directions, respectively. Two Langevin thermostats with a temperature difference of 20 K are used to establish temperature gradient along axial direction. Noting that the same definition of thickness for cross-sectional area (CSA) should be used when compare heat transfer capability of low dimensional material [42]. The CSA of nanotube is defined as a ring with thickness of 6.16 Å, which is the interlayer distance of $SLMoS_2$. To overcome the statistical error, all results are averaged over five independent simulations with different initial conditions. (NEMD simulation details are given in supplementary material)

3. Results and discussion

Firstly, thermal conductivity of MoS_2NT with a diameter of 7 nm and a length of 10 nm is calculated at 300 K, and the result is depicted in Fig. 2a as an illustration of the NEMD method. By linear fitting temperature profile (the red line), temperature gradient is obtained to calculate thermal conductivity. Since temperature usually play a critical role in thermal transport, dependence of thermal conductivity on temperature is further investigated. Debye temperature of $SLMoS_2$ is reported as 278 K [16], which can be assumed equal to that of MoS_2NT. So thermal conductivity of MoS_2NT is calculated in the temperature range from 200 to 400 K. As shown in Fig. 2b, there is no obvious difference between the thermal conductivity of ANT and ZNT. An approximate value of 16 $Wm^{-1}K^{-1}$ is obtained for both ANT and ZNT at room temperature, which is on the same order of magnitude as the results of $SLMoS_2$ [13,14] and aligned CNT-PE composites [43] with the same length. In order to compare, thermal conductivity of the corresponding nanoribbon is calculated as well. It shows that thermal conductivity of ZNT is almost equal to that of zigzag nanoribbon, however the value of ANT is smaller than that of armchair nanoribbon. The reason is that more strain is introduced in the specific structure of ANT by curvature, which lead to more phonon scattering. Moreover, thermal conductivity of both ANT and ZNT decrease when temperature increases from 200 K to 400 K. It shows that thermal conductivity can be well fitted by the $\sim T^{-1}$ function, which is attributed to the enhancement of Umklapp phonon-phonon scattering at higher temperature. The similar result is also found by previous study on CNT [44].

Then, length dependence of thermal conductivity is studied at room temperature, where the diameter is fixed as 7 nm. As shown in Fig. 2c, thermal conductivity of both ANT and ZNT increase with length ranging from 10 to 320 nm. With length up to 320 nm, the

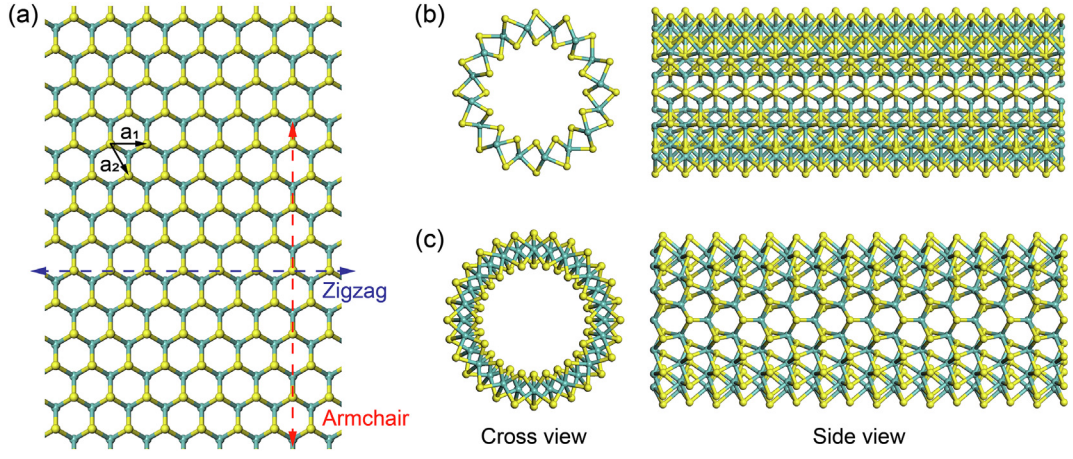

Fig. 1. Schematic construction of MoS_2NT from single layer $SLMoS_2$. (a) Hexagonal $SLMoS_2$ lattice with indication of primitive vectors and the rolling directions for ANT and ZNT. (b and c) The cross and side view of (8,8) ANT and (14,0) ZNT. Yellow and green spheres represent S and Mo atoms respectively.

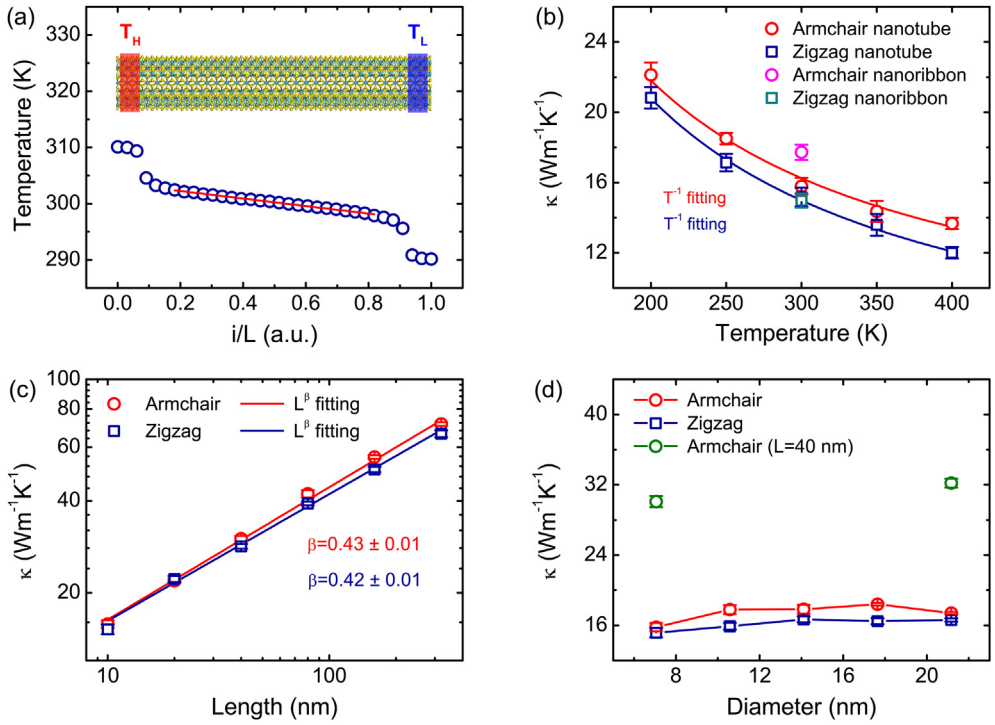

Fig. 2. (a) The schematic of MoS_2NT and linear fitting of the temperature profile obtained from averaging during NEMD simulation; Thermal conductivity of MoS_2NT with different chirality versus (b) temperature (the diameter and length are set as 7 nm and 10 nm respectively), (c) length (the diameter is set as 7 nm) and (d) diameter (the length is set as 10 nm) at 300 K.

values are obtained as high as 71 ± 1 Wm^{-1} K^{-1} and 66 ± 2 Wm^{-1} K^{-1} for ANT and ZNT respectively. When length is shorter than phonon mean free path, the low-energy phonon density is very small, and phonon-phonon interaction can be neglected so that phonons transport ballistically. With the increase of length, more and more (low energy, long wavelength) phonons are excited, which results in the linear increase of thermal conductivity. When length is longer than phonon mean free path, the phonon phonon scattering plays a key role in the process of phonon transport. Based on the theoretical studies on low-dimensional lattice model [45,46], the anomalous heat diffusion induced by super diffusive phonon transport is responsible for the divergent thermal conductivity. Moreover, thermal conductivity is fitted to diverge with length as $\kappa \propto L^{\beta}$, β is obtained as 0.43 ± 0.01 and 0.42 ± 0.01 for ANT and ZNT respectively, which is consistent with the previous value 0.4 obtained from CNT [47]. The similar length effect was also observed in the previous studies on CNT [44], $SLMoS_2$ [14] and silicon nanowires [38,48].

Furthermore, diameter dependence of thermal conductivity is studied at room temperature, where the length is fixed as 10 nm. As shown in Fig. 2d, thermal conductivity of both ANT and ZNT are almost unchanged when diameter increases from 7 to 21 nm. To eliminate the influence of insufficient nanotube length, thermal conductivity of ANT with a length of 40 nm is calculated at two different diameters. The result shows that thermal conductivity of longer nanotube is still almost unchanged when diameter increases from 7 to 21 nm. Therefore, it indicates that thermal conductivity of MoS_2NT has no obvious dependence on diameter, it converges to a constant when diameter is large. As we know, when diameter increases from small to large, thermal conductivity increases because more phonon modes are excited and phonon scattering induced by curvature is weaken. However, continuing increase of diameter cannot enhance thermal conductivity due to the increase of phonon-phonon scattering. On the other hand, unlike the mechanism of length dependent thermal conductivity, increasing diameter cannot increase the phonon mean free path along axial direction. Therefore, thermal conductivity of nanotube should converge with the diameter. Our result is similar to the thermal conductivity of CNT, which increases firstly and then converges when diameter is larger than 7 nm [49].

Besides temperature and size effect, strain effect on thermal conductivity is investigated for both ANT and ZNT, the diameter and length are fixed as 7 nm and 10 nm respectively. Due to the limitation of structural stability, the strain is applied along the axial direction of nanotube, ranging from −0.03 to 0.03 for ANT and −0.03 to 0.09 for ZNT. As shown in Fig. 3a, ANT can only tolerate strain in a small range and thermal conductivity only slightly decreases with strain in that range. In contrast, thermal conductivity of ZNT is significantly influenced by strain. It decreases almost linearly with tensile strain, but abruptly reduces by about fifty percent when strain is larger than 0.06. That is, the strain effect on thermal conductivity has a strong chirality dependence.

To understand the underlying mechanism of the strain effect on thermal conductivity, phonon density of state (PDOS) in axial direction is calculated for different strained nanotube. The PDOS spectra are obtained through Fourier transform of velocity. As shown in Fig. 3b, the lower frequency phonon modes are not sensitive to strain. Differently, higher frequency modes shift to low frequency region when nanotube undergoes tensile strain, which indicates that phonon dispersion is compressed to lower frequency region. Based on $\kappa = cv^2\tau/3$, reduction of thermal conductivity is related to the decrease of phonon group velocity and relaxation time. To show it clearly, we calculate the phonon dispersion by the general utility lattice program (GULP) [50]. Fig. 3c shows that the phonon modes shift to the lower frequency region, which is consistent with that indicated by PDOS. As shown in Fig. 3d, the phonon group velocity of nanotube at different strain are calculated. It is obvious that group velocity significantly decreases when nanotube is stretched, especially for the low frequency part, which contribute more to thermal conductivity. Particularly for the

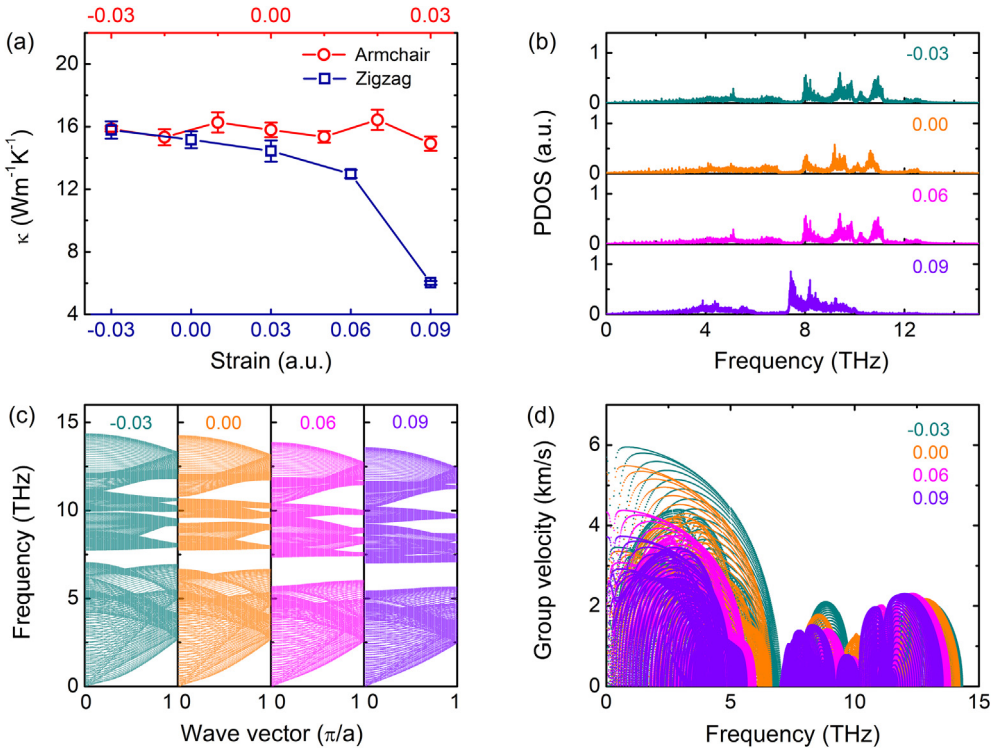

Fig. 3. (a) Thermal conductivity of MDNT with different chirality versus strain at room temperature, the diameter and length are set as 7 nm and 10 nm respectively; (b) Normalized PDOS along axial direction for different strained ZNT. (c) Phonon dispersion relation for different strained ZNT; (d) Phonon group velocity versus frequency for different strained ZNT.

acoustic phonons that mainly contribute to thermal conductivity, their group velocity is significantly reduced from about 4.3 to 3.8 km/s when strain increases from 0.06 to 0.09, which is the main reason for the abrupt decrease of thermal conductivity. On the other hand, phase space is changed and anharmonicity is introduced by strain, which enhance the phonon scattering so that phonon relaxation time is reduced. Therefore, the significant reduction of thermal conductivity is observed when strain is larger than 0.06. All in all, the decreasing thermal conductivity is attributed to the reduction of group velocity and phonon relaxation time induced by strain.

4. Conclusion

In general, the thermal conductivity of MoS_2NT is systematically studied by NEMD simulations. The result shows that thermal conductivity decreases with temperature as T^{-1} from 200 to 400 K, which indicates the dominant three-phonon scattering mechanism. Moreover, thermal conductivity has a strong dependence on length and the value diverges as L^{β} ($\beta \sim 0.4$) from 10 to 320 nm. However, it has a weak dependence on diameter. More importantly, it is found that the strain can dramatically reduce thermal conductivity of ZNT rather than that of ANT. That is, there is a chirality-dependent strain effect. By calculating the PDOS and phonon dispersion relations, the strain effect on thermal conductivity is attributed to the decrease of phonon group velocity induced by strain, which makes phonon modes drift to low-frequency region. Our results demonstrate the possibility to modulate thermal conductivity of MoS_2NT through temperature, length and strain. This work offers useful insights into the fundamental mechanisms that govern the thermal conductivity, which can be used for the thermal management of low dimensional materials in optical, electronic and thermoelectrical devices.

Declaration of Competing Interest

There are no conflicts of interest to declare.

Acknowledgements

This work is financially supported by the National Natural Science Foundation of China (No. 51576076 and No. 51711540031), the Natural Science Foundation of Hubei Province (No. 2017CFA046), and the Fundamental Research Funds for the Central Universities, HUST (No. 2019kfyRCPY045). We are grateful to Meng An, Xiao Wan, Wentao Feng and Shichen Deng for useful discussions. The authors thank the National Supercomputing Center in Tianjin (NSCC-TJ) and China Scientific Computing Grid (ScGrid) for providing assistance in computations.

Appendix A. Supplementary material

Supplementary data to this article can be found online at https://doi.org/10.1016/j.ijheatmasstransfer.2019.118719.

References

[1] G. Eda, H. Yamaguchi, D. Voiry, T. Fujita, M. Chen, M. Chhowalla, Photoluminescence from chemically exfoliated MoS2, Nano Lett. 11 (12) (2011) 5111–5116.
[2] A. Splendiani, L. Sun, Y. Zhang, T. Li, J. Kim, C.-Y. Chim, G. Galli, F. Wang, Emerging photoluminescence in monolayer MoS2, Nano Lett. 10 (4) (2010) 1271–1275.
[3] S. Bertolazzi, J. Brivio, A. Kis, Stretching and breaking of ultrathin MoS2, ACS Nano 5 (12) (2011) 9703–9709.
[4] A. Castellanos-Gomez, M. Poot, G.A. Steele, H.S. van der Zant, N. Agraït, G. Rubio-Bollinger, Elastic properties of freely suspended MoS2 nanosheets, Adv. Mater. 24 (6) (2012) 772–775.
[5] K.F. Mak, C. Lee, J. Hone, J. Shan, T.F. Heinz, Atomically thin MoS 2: a new direct-gap semiconductor, Phys. Rev. Lett. 105 (13) (2010) 136805.

[6] W. Choi, M.Y. Cho, A. Konar, J.H. Lee, G.B. Cha, S.C. Hong, S. Kim, J. Kim, D. Jena, J. Joo, High-detectivity multilayer MoS2 phototransistors with spectral response from ultraviolet to infrared, Adv. Mater. 24 (43) (2012) 5832–5836.

[7] H.S. Lee, S.-W. Min, Y.-G. Chang, M.K. Park, T. Nam, H. Kim, J.H. Kim, S. Ryu, S. Im, MoS2 nanosheet phototransistors with thickness-modulated optical energy gap, Nano Lett. 12 (7) (2012) 3695–3700.

[8] J. Pu, Y. Yomogida, K.-K. Liu, L.-J. Li, Y. Iwasa, T. Takenobu, Highly flexible MoS2 thin-film transistors with ion gel dielectrics, Nano Lett. 12 (8) (2012) 4013–4017.

[9] J. He, D. Li, Y. Ying, H. Zhou, P. Zhou, G. Zhang, The ultrahigh quantum thermal conductance of hydrogenated boron nanotubes, Physica Status Solidi (b) 256 (8) (2019) 1900122.

[10] M. Remskar, A. Mrzel, Z. Skraba, A. Jesih, M. Ceh, J. Demšar, P. Stadelmann, F. Lévy, D. Mihailovic, Self-assembly of subnanometer-diameter single-wall MoS₂ nanotubes, Science 292 (5516) (2001) 479.

[11] J. Chen, S.-L. Li, Q. Xu, K. Tanaka, Synthesis of open-ended MoS2 nanotubes and the application as the catalyst of methanation, Chem. Commun. 16 (2002) 1722–1723.

[12] R. Yan, J.R. Simpson, S. Bertolazzi, J. Brivio, M. Watson, X. Wu, A. Kis, T. Luo, A.R. Hight Walker, H.G. Xing, Thermal conductivity of monolayer molybdenum disulfide obtained from temperature-dependent raman spectroscopy, ACS Nano 8 (1) (2014) 986–993.

[13] Z. Jin, Q. Liao, H. Fang, Z. Liu, W. Liu, Z. Ding, T. Luo, N. Yang, A revisit to high thermoelectric performance of single-layer MoS 2, Sci. Rep. 5 (2015) 18342.

[14] X. Wu, N. Yang, T. Luo, Unusual isotope effect on thermal transport of single layer molybdenum disulphide, Appl. Phys. Lett. 107 (19) (2015) 191907.

[15] Z. Ding, Q.-X. Pei, J.-W. Jiang, Y.-W. Zhang, Manipulating the thermal conductivity of monolayer MoS2 via lattice defect and strain engineering, J. Phys. Chem. C 119 (28) (2015) 16358–16365.

[16] B. Peng, H. Zhang, H. Shao, Y. Xu, X. Zhang, H. Zhu, Towards intrinsic phonon transport in single-layer MoS2, Ann. Phys. 528 (6) (2016) 504–511.

[17] M. Yarali, X. Wu, T. Gupta, D. Ghoshal, M. Anastassios, Effects of defects on the temperature dependent thermal conductivity of suspended monolayer molybdenum disulfide grown by chemical vapor deposition, Adv. Funct. Mater. 27 (46) (2017) 1704357.

[18] E.W. Bucholz, S.B. Sinnott, Mechanical behavior of MoS2 nanotubes under compression, tension, and torsion from molecular dynamics simulations, J. Appl. Phys. 112 (12) (2012) 123510.

[19] Z. Ahadi, M. Shadman Lakmehsari, S. Kumar Singh, J. Davoodi, Stability and thermal behavior of molybdenum disulfide nanotubes: Nonequilibrium molecular dynamics simulation using REBO potential, J. Appl. Phys. 122 (22) (2017).

[20] H. Meng, X. Yu, H. Feng, Z. Xue, N. Yang, Superior thermal conductivity of poly (ethylene oxide) for solid-state electrolytes: a molecular dynamics study, Int. J. Heat Mass Transf. 137 (2019) 1241–1246.

[21] X. Wan, W. Feng, Y. Wang, H. Wang, X. Zhang, C. Deng, N. Yang, Materials discovery and properties prediction in thermal transport via materials informatics: a mini-review, Nano Lett. (2019).

[22] M. An, B. Demir, X. Wan, H. Meng, N. Yang, T.R. Walsh, Predictions of thermo-mechanical properties of cross-linked polyacrylamide hydrogels using molecular simulations, Adv. Theory Simulations 2 (3) (2019) 1800153.

[23] Y. Kawagoe, D. Surblys, H. Matsubara, G. Kikugawa, T. Ohara, Construction of polydisperse polymer model and investigation of heat conduction: a molecular dynamics study of linear and branched polyethylenimine, Polymer 121721 (2019).

[24] Y. Guo, D. Surblys, Y. Kawagoe, H. Matsubara, X. Liu, T. Ohara, A molecular dynamics study on the effect of surfactant adsorption on heat transfer at a solid-liquid interface, Int. J. Heat Mass Transf. 135 (2019) 115–123.

[25] D. Ma, X. Wan, N. Yang, Unexpected thermal conductivity enhancement in pillared graphene nanoribbon with isotopic resonance, Phys. Rev. B 98 (24) (2018) 245420.

[26] M. An, Q. Song, X. Yu, H. Meng, D. Ma, R. Li, Z. Jin, B. Huang, N. Yang, Generalized two-temperature model for coupled phonons in nanosized graphene, Nano Lett. 17 (9) (2017) 5805–5810.

[27] D. Ma, H. Ding, H. Meng, L. Feng, Y. Wu, J. Shiomi, N. Yang, Nano-cross-junction effect on phonon transport in silicon nanowire cages, Phys. Rev. B 94 (16) (2016) 165434.

[28] J.-W. Jiang, N. Yang, B.-S. Wang, T. Rabczuk, Modulation of thermal conductivity in kinked silicon nanowires: phonon interchanging and pinching effects, Nano Lett. 13 (4) (2013) 1670–1674.

[29] S. Plimpton, Fast parallel algorithms for short-range molecular dynamics, J. Comput. Phys. 117 (1) (1995) 1–19.

[30] Z. Ding, M. An, S. Mo, X. Yu, Z. Jin, Y. Liao, K. Esfarjani, J.-T. Lü, J. Shiomi, N. Yang, Unexpectedly high cross-plane thermoelectric performance of layered carbon nitrides, J. Mater. Chem. A 7 (5) (2019) 2114–2121.

[31] G. Xie, D. Ding, G. Zhang, Phonon coherence and its effect on thermal conductivity of nanostructures, Adv. Phys.: X 3 (1) (2018) 1480417.

[32] L. Cui, Y. Feng, J. Tang, P. Tan, X. Zhang, Heat conduction in coaxial nanocables of Au nanowire core and carbon nanotube shell: a molecular dynamics simulation, Int. J. Therm. Sci. 99 (2016) 64–70.

[33] Y. Feng, H. Zou, L. Qiu, X. Zhang, Size effect on the thermal conductivity of octadecanoic acid: a molecular dynamics study, Comput. Mater. Sci. 158 (2019) 14–19.

[34] R. Su, X. Zhang, Size effect of thermal conductivity in monolayer graphene, Appl. Therm. Eng. 144 (2018) 488–494.

[35] F.H. Stillinger, T.A. Weber, Computer simulation of local order in condensed phases of silicon, Phys. Rev. B 31 (8) (1985) 5262.

[36] D. Ma, A. Arora, S. Deng, G. Xie, J. Shiomi, N. Yang, Quantifying phonon particle and wave transport in silicon nanophononic metamaterial with cross junction, Mater. Today Phys. 8 (2019) 56–61.

[37] L. Yang, N. Yang, B. Li, Extreme low thermal conductivity in nanoscale 3D Si phononic crystal with spherical pores, Nano Lett. 14 (4) (2014) 1734–1738.

[38] N. Yang, G. Zhang, B. Li, Violation of Fourier's law and anomalous heat diffusion in silicon nanowires, Nano Today 5 (2) (2010) 85–90.

[39] N. Yang, G. Zhang, B. Li, Ultralow thermal conductivity of isotope-doped silicon nanowires, Nano Lett. 8 (1) (2008) 276–280.

[40] J.-W. Jiang, Parametrization of Stillinger-Weber potential based on valence force field model: application to single-layer MoS2 and black phosphorus, Nanotechnology 26 (31) (2015) 315706.

[41] W.C. Swope, H.C. Andersen, P.H. Berens, K.R. Wilson, A computer simulation method for the calculation of equilibrium constants for the formation of physical clusters of molecules: Application to small water clusters, J. Chem. Phys. 76 (1) (1982) 637–649.

[42] X. Wu, V. Varshney, J. Lee, Y. Pang, A.K. Roy, T. Luo, How to characterize thermal transport capability of 2D materials fairly? – Sheet thermal conductance and the choice of thickness, Chem. Phys. Lett. 669 (2017) 233–237.

[43] Q. Liao, Z. Liu, W. Liu, C. Deng, N. Yang, Extremely high thermal conductivity of aligned carbon nanotube-polyethylene composites, Sci. Rep. 5 (2015) 16543.

[44] S. Maruyama, A molecular dynamics simulation of heat conduction of a finite length single-walled carbon nanotube, Microscale Thermophys. Eng. 7 (1) (2003) 41–50.

[45] B. Li, J. Wang, Anomalous Heat Conduction and Anomalous Diffusion in One-Dimensional Systems, Phys. Rev. Lett. 91 (4) (2003) 044301.

[46] B. Li, J. Wang, L. Wang, G. Zhang, Anomalous heat conduction and anomalous diffusion in nonlinear lattices, single walled nanotubes, and billiard gas channels, Chaos 15 (1) (2005) 015121, https://doi.org/10.1063/1.1832791.

[47] G. Zhang, B. Li, Thermal conductivity of nanotubes revisited: effects of chirality, isotope impurity, tube length, and temperature, J. Chem. Phys. 123 (11) (2005) 114714.

[48] S.-C. Wang, X.-G. Liang, X.-H. Xu, T. Ohara, Thermal conductivity of silicon nanowire by nonequilibrium molecular dynamics simulations, J. Appl. Phys. 105 (1) (2009) 014316.

[49] L. Lindsay, D. Broido, N. Mingo, Diameter dependence of carbon nanotube thermal conductivity and extension to the graphene limit, Phys. Rev. B 82 (16) (2010) 161402.

[50] J.D. Gale, A.L. Rohl, The general utility lattice program (GULP), Mol. Simul. 29 (5) (2003) 291–341.